Regulation of antibacterial defense in the small intestine by the nuclear bile acid receptor

Takeshi Inagaki*, Antonio Moschetta†‡, Youn-Kyoung Lee*, Li Peng*, Guixiang Zhao*, Michael Downes§, Ruth T. Yu§, John M. Shelton¶, James A. Richardson¶, Joyce J. Repa‖, David J. Mangelsdorf†‡, and Steven A. Kliewer*†**

Departments of *Molecular Biology, †Pharmacology, ¶Pathology, and ‖Physiology and ‡Howard Hughes Medical Institute, University of Texas Southwestern Medical Center, Dallas, TX 75390; and §Gene Expression Laboratory, The Salk Institute for Biological Studies, La Jolla, CA 92037

Edited by Bert W. O'Malley, Baylor College of Medicine, Houston, TX, and approved December 23, 2005 (received for review November 3, 2005)

Obstruction of bile flow results in bacterial proliferation and mucosal injury in the small intestine that can lead to the translocation of bacteria across the epithelial barrier and systemic infection. These adverse effects of biliary obstruction can be inhibited by administration of bile acids. Here we show that the farnesoid X receptor (FXR), a nuclear receptor for bile acids, induces genes involved in enteroprotection and inhibits bacterial overgrowth and mucosal injury in ileum caused by bile duct ligation. Mice lacking FXR have increased ileal levels of bacteria and a compromised epithelial barrier. These findings reveal a central role for FXR in protecting the distal small intestine from bacterial invasion and suggest that FXR agonists may prevent epithelial deterioration and bacterial translocation in patients with impaired bile flow.

bacteria | biliary obstruction | epithelial barrier | ileum

Bile acids are amphipathic cholesterol metabolites that are synthesized in the liver, stored in the gallbladder, and released after feeding into the small intestine, where they are crucial for the absorption of lipids and lipid-soluble vitamins (1). In addition to their role in digestion, bile acids affect the microflora and integrity of the small intestine. Obstruction of bile flow in humans or rodents causes proliferation of intestinal bacteria and mucosal injury, which can lead to bacterial translocation across the mucosal barrier and systemic infection (2). Oral administration of bile acids inhibits the bacterial overgrowth and translocation caused by biliary obstruction in rodents (3, 4). Moreover, preoperative oral administration of bile acids blocks endotoxemia in patients with obstructive jaundice (5–7). The mechanisms underlying the beneficial actions of bile acids are not known.

The farnesoid X receptor (FXR) is a member of the steroid/thyroid hormone receptor family of ligand-activated transcription factors that is activated by bile acids including cholic acid and chenodeoxycholic acid (8). FXR modulates gene expression by binding as a heterodimer with the retinoid X receptors to DNA response elements in the regulatory regions of target genes. FXR is much studied in liver, where it regulates a program of genes involved in maintaining bile acid homeostasis (8). FXR is also expressed in the intestine, where it regulates several genes, including the ileal bile acid binding protein and fibroblast growth factor 15 (9–12). However, little is known about the overarching function of FXR in the gut.

In this report we have examined the role of FXR in the ileum. We demonstrate that it plays a crucial role in preventing bacterial overgrowth and maintaining the integrity of the intestinal epithelium.

Results

Real-time quantitative PCR (RTQ-PCR) was used to measure FXR mRNA concentrations in duodenum, jejunum, ileum, colon, and liver. FXR was expressed in each of these tissues, with highest mRNA levels in ileum (Fig. 1*A*). A previous study showed that FXR is expressed in the villus epithelium in late-stage mouse embryos (13). Consistent with this finding, *in situ* hybridization analysis with ileum sections revealed that FXR is expressed in the villus epithelium in adult mouse ileum, with highest expression in the intervillus regions (Fig. 1*B*). Little or no FXR mRNA was detected in the crypts of Lieberkühn, lamina propria, and tunica muscularis.

To gain insight into the function of FXR in the small intestine, transcriptional profiling experiments were done by using mice lacking the gene encoding sterol 27-hydroxylase (CYP27), a key enzyme for bile acid synthesis. The CYP27-knockout (KO) mice produce only low levels of bile acids and thus are essentially devoid of endogenous FXR agonists (14). RNA was prepared from ileal mucosa of CYP27-KO mice administered either the potent, synthetic FXR agonist GW4064 (15) or vehicle for 14 h. Microarray analysis yielded a list of 15 genes whose expression was changed ≥2-fold by GW4064 administration (Table 1). Among these were the established FXR target genes small heterodimer partner (*Shp*), fibroblast growth factor 15 (*Fgf15*), and ileal bile acid binding protein (*Ibabp*), which encode proteins involved in bile acid homeostasis (9–12, 16, 17). Interestingly, several of the other genes in Table 1 have established roles in mucosal defense in the intestine. NO, the product of inducible NO synthase (iNOS), has direct antimicrobial effects and regulates many different aspects of the innate immune response, including mucus secretion, vascular tone, and epithelial barrier function (18, 19). The proinflammatory cytokine IL18 stimulates resistance to an array of pathogens, including intracellular and extracellular bacteria and mycobacteria, and appears to have a protective role during the early, acute phase of mucosal immune response (20, 21). Angiogenin (ANG1) and RNase A family member 4 (RNASE4) are closely related proteins that arise by differential splicing from a common gene locus (22). Although the function of RNASE4 is not established, ANG1 is part of the acute phase response to infection and has potent antibacterial and antimycotic actions (23). Carbonic anhydrase 12 (CAR12) is a member of a family of proteins involved in the maintenance of pH and ion balance (24). The regulation of all of these genes by FXR was confirmed by RTQ-PCR by using WT, CYP27-KO, and FXR-KO mice administered either GW4064 or vehicle (Fig. 5, which is published as supporting information on the PNAS web site). Notably, FXR had different effects on different genes. For example, activation of FXR had little or no effect on *Ibabp* or *iNos* expression in WT mice, but its elimination caused a marked decrease in the basal expression of these genes (Fig. 5). In contrast, FXR activation induced *Il18* but did not contribute to its basal expression (Fig. 5). Based on these data, the

Conflict of interest statement: No conflicts declared.

This paper was submitted directly (Track II) to the PNAS office.

Abbreviations: FXR, farnesoid X receptor; RTQ-PCR, real-time quantitative PCR; CYP27, sterol 27-hydroxylase; KO, knockout; BDL, bile duct ligation; iNOS, inducible NO synthase.

**To whom correspondence should be addressed at: University of Texas Southwestern Medical Center, 5323 Harry Hines Boulevard, Room ND9.502, Dallas, TX 75390-9041. E-mail: steven.kliewer@utsouthwestern.edu.

www.pnas.org/cgi/doi/10.1073/pnas.0509592103

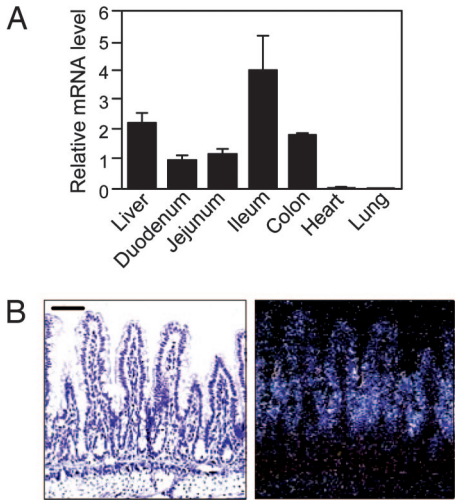

Fig. 1. FXR is expressed in the intestine. (*A*) Total RNA was prepared from the indicated tissues of WT mice ($n = 5$), and FXR mRNA concentrations were measured by RTQ-PCR by using cyclophilin as the internal control. Data represent the mean ± SEM and are plotted as fold change relative to mRNA levels in duodenum. (*B*) *In situ* hybridization analysis was performed with an ^{35}S-labeled FXR antisense riboprobe and transverse sections of distal ileum from WT mice. Bright-field (*Left*) and dark-field (*Right*) images are shown. (Scale bar: 50 μm.)

possibility that *Il18* induction by FXR is pharmacological rather than physiological cannot be excluded.

Decreased bile secretion in rodents by either ligation of the common bile duct or induction of cirrhosis causes changes in the small intestine, including bacterial overgrowth and translocation across the mucosal barrier (3, 4, 25–30). Oral administration of bile acids inhibits these effects (3, 4). The genes regulated by FXR in ileum suggested that it might contribute to the enteroprotective actions of bile acids. To test this hypothesis, groups of WT and FXR-KO mice (31) were administered either GW4064 or vehicle for 2 days and then subjected to bile duct ligation (BDL) or sham operation. After 5 days, during which GW4064 or vehicle treatment was continued, the mice were killed and their intestines were analyzed for FXR target gene expression and bacterial content.

Table 1. Genes regulated by FXR agonist GW4064 in ileum

Average ratio	Unigene accession no.	Gene title
83	Mm.3904	Fibroblast growth factor 15
43	Mm.34209	Small heterodimer partner
11	Mm.140210	Ubiquitin D
4.0	Mm.2893	iNOS
2.8	Mm.175173	RNase A family 4
2.8	Mm.215171	Translent receptor potential cation channel
2.6	Mm.12914	Ubiquitin-specific protease 2
2.3	Mm.202665	Angiogenin
2.3	Mm.21397	Carbonic anhydrase 12
2.2	Mm.1410	IL18
2.1	Mm.142716	Ileal bile acid binding protein
2.0	Mm.116904	Solute carrier family 26, member 3
2.0	Mm.33987	Dual adaptor for phosphotyrosine
2.0	Mm.29988	Peroxisomal trans-2-enoyl-CoA reductase
−3.7	Mm.34289	Histocompatibility 2, blastocyst (H2-Q10)

CYP27-KO mice were treated for 14 h with vehicle or GW4064. RNA was prepared from ileum and used in transcriptional profiling studies. Average ratio represents the fold regulation in RNA prepared from GW4064-treated mice relative to vehicle-treated mice.

As expected, BDL caused jaundice manifested by increased total serum bilirubin concentrations in both WT and FXR-KO mice (Fig. 2*A*). GW4064 administration had no effect on total serum bilirubin concentrations in BDL mice. BDL also had marked effects on genes regulated by FXR in ileum. In WT mice, expression of *Fgf15*, *Shp*, *Ang1*, *Car12*, and *Ibabp* was reduced by BDL (Fig. 2). GW4064 administration increased expression of these genes in BDL mice to levels above those seen in sham-operated animals. None of these genes was induced by GW4064 in FXR-KO mice. In contrast, the *iNos* and *Il18* genes showed a more complex expression pattern (Fig. 2 *D* and *G*). Although both genes are induced by FXR (Fig. 5), there was a trend toward increased expression in BDL mice that occurred in an FXR-independent fashion (Fig. 2 *D* and *G*). Because both *iNos* and *Il18* are induced by proinflammatory stimuli, including lipopolysaccharide and various cytokines (32, 33), this likely reflects regulation of these genes by additional signaling pathways that are activated by BDL.

The effect of BDL and GW4064 treatment on the bacterial content of ileum and cecum was assessed. As expected, BDL increased the number of aerobic and anaerobic bacteria in the ileum and cecum of WT mice (Fig. 3 *A–D*). The increase was particularly pronounced for aerobic bacteria (Fig. 3 *A* and *C*). Notably, bacterial overgrowth in the lumen of both tissues was completely blocked by administration of GW4064 to BDL mice (Fig. 3 *A–D*).

To determine whether FXR is required for the antibacterial actions of GW4064, the same set of experiments was performed in FXR-KO mice. Two important differences were seen between WT and FXR-KO mice. First, GW4064 did not decrease aerobic or anaerobic bacteria counts in the ileum or cecum of FXR-KO mice (Fig. 3 *A–D*). The reason for the marked variability in the bacterial counts in BDL FXR-KO mice is not known. Nevertheless, these data demonstrate that the antibacterial actions of GW4064 require FXR. Second, sham-operated FXR-KO mice had significantly higher aerobic bacteria counts than sham-operated, WT mice (Fig. 3 *A* and *C*). These data support a role for FXR in suppressing bacterial proliferation under normal physiologic conditions. Because FXR-KO mice have reduced hepatic bile salt export pump (ABCB11) expression (31), decreased bile acid concentrations in the intestinal lumen of these animals may contribute to the bacterial overgrowth. In complementary *in vitro* experiments, GW4064 had no bacteriostatic effects in aerobic cultures of ileal contents even at 10 μM concentrations (data not shown), demonstrating that GW4064 itself does not have direct antibacterial activity.

As a measure of bacterial translocation across the mucosal barrier, bacteria were also quantified in the mesenteric lymph node complex for each of the treatment groups (Fig. 3 *E* and *F*). The pattern for the bacterial counts was similar to that seen for bacterial overgrowth in the ileum and cecum. In WT mice, BDL resulted in an increase in bacterial number in the mesenteric lymph node complex, and GW4064 treatment completely inhibited this effect. The effect was particularly pronounced for aerobic bacteria (Fig. 3*E*). FXR-KO mice had ≈10-fold higher levels of aerobic bacteria in mesenteric lymph nodes as compared with WT animals (Fig. 3*E*; note differences in scales for WT and FXR-KO mice), and BDL caused a trend toward increased bacterial counts (Fig. 3 *E* and *F*). This trend was not reversed by GW4064 administration (Fig. 3 *E* and *F*).

The increase in *in vivo* bacterial translocation suggested that BDL causes a disruption of the intestinal barrier function that is inhibited by FXR. To examine barrier integrity, immunostaining was done for occludin, a component of the epithelial tight

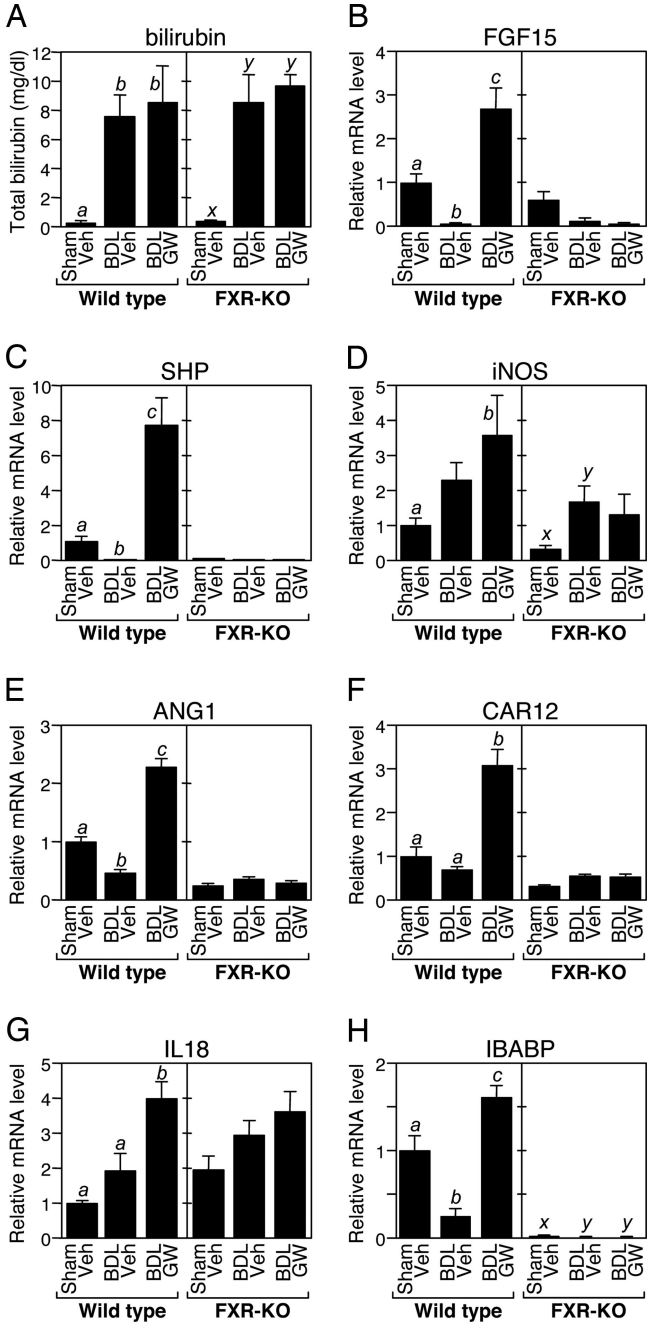

Fig. 2. Effects of BDL and GW4064 on serum bilirubin concentrations and FXR-regulated genes. (*A*) Total bilirubin was measured in serum from WT and FXR-KO mice (n = 5–9) subjected to sham operation and vehicle (Veh) treatment, BDL and vehicle treatment, or BDL and GW4064 (GW) treatment. The presence of different lowercase letters indicates statistical significance ($P <$ 0.01) within each strain. (*B–H*) Total RNA was prepared from ileum of WT and FXR-KO mice (n = 5–9) subjected to sham operation and vehicle (Veh) treatment, BDL and vehicle treatment, or BDL and GW4064 (GW) treatment. Expression of the indicated genes was measured by RTQ-PCR by using cyclophilin as the internal control. Data represent the mean ± SEM and are plotted as fold change relative to mRNA levels in sham-operated mice treated with vehicle. The presence of different lowercase letters indicates statistical significance ($P < 0.05$) within each strain.

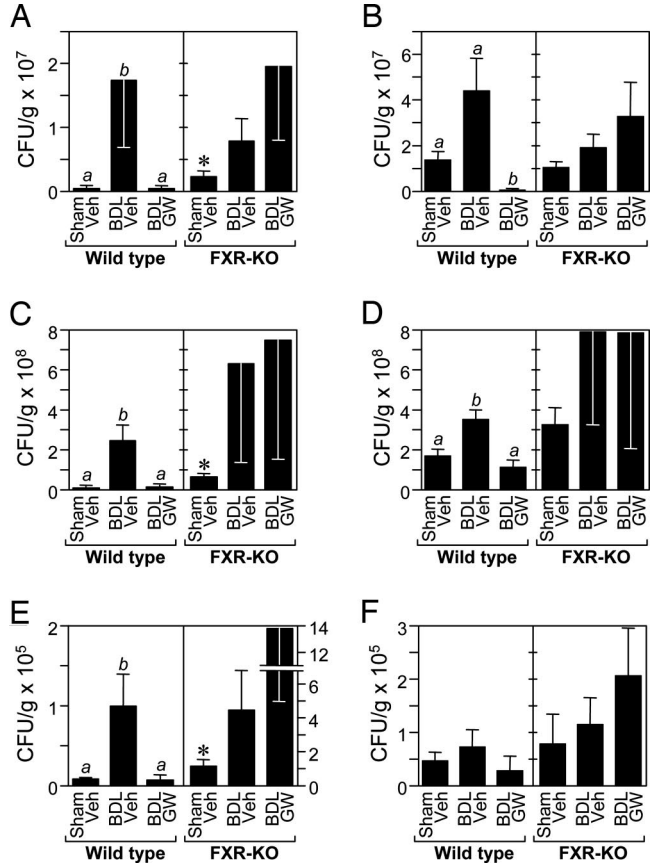

Fig. 3. FXR activation blocks bacterial overgrowth and translocation. Aerobic (*A*, *C*, and *E*) and anaerobic (*B*, *D*, and *F*) bacteria were quantified in ileum (*A* and *B*), cecum (*C* and *D*), and mesenteric lymph node complexes (*E* and *F*) of WT and FXR-KO mice (n = 5–9) subjected to sham operation and vehicle (Veh) treatment, BDL and vehicle treatment, or BDL and GW4064 (GW) treatment. Data represent the mean ± SEM. The presence of different lowercase letters indicates statistical significance ($P < 0.05$) within each strain. Asterisks indicate statistical significance ($P < 0.05$) between sham-operated, vehicle-treated FXR-KO mice and sham-operated, vehicle-treated WT mice. CFU, colony-forming units.

junctions. In the villus epithelium of WT mice, occludin staining was continuous except where interrupted by the normal presence of mucus-secreting goblet cells (Fig. 4*A*). In contrast, many enterocytes in the BDL mice expressed little or no occludin (Fig. 4*A*). Consistent with these data, transmission electron microscopy revealed large ruptures in the mucosal surface of BDL WT mice, with bacteria penetrating deep into the epithelium (Fig. 4 *C* and *D*). Hematoxylin and eosin staining revealed that the breakdown in barrier function was accompanied by dilated lymphatics and a pronounced interstitial edema, as previously described (Fig. 4*B*) (3, 25, 26, 34). In many villi, the severity of the edema caused separation of the villus epithelium from the underlying lamina propria (Fig. 4*B*). Bacteria were seen within edematous areas by electron microscopy (Fig. 4*D*). Consistent with the edema resulting from an inflammatory response, there was a marked increase in the number of neutrophils infiltrating the villi of BDL mice (Fig. 4*G*). Neutrophils are known to contribute to epithelial permeability in inflammatory diseases of the intestine (35).

GW4064 prevented the pathological effects caused by BDL. Ilea from BDL mice administered GW4064 showed a more continuous pattern of occludin immunostaining (Fig. 4*A*), little or no edema (Fig. 4*B*), and a reduction in the number of neutrophils to the level seen in sham-operated mice (Fig. 4*G*). Virtually no mucosal damage was detected in electron microscopy studies done by using tissue from GW4064-treated mice (data not shown). Thus, activation of FXR prevents deterioration of the epithelial barrier and the accompanying inflamma-

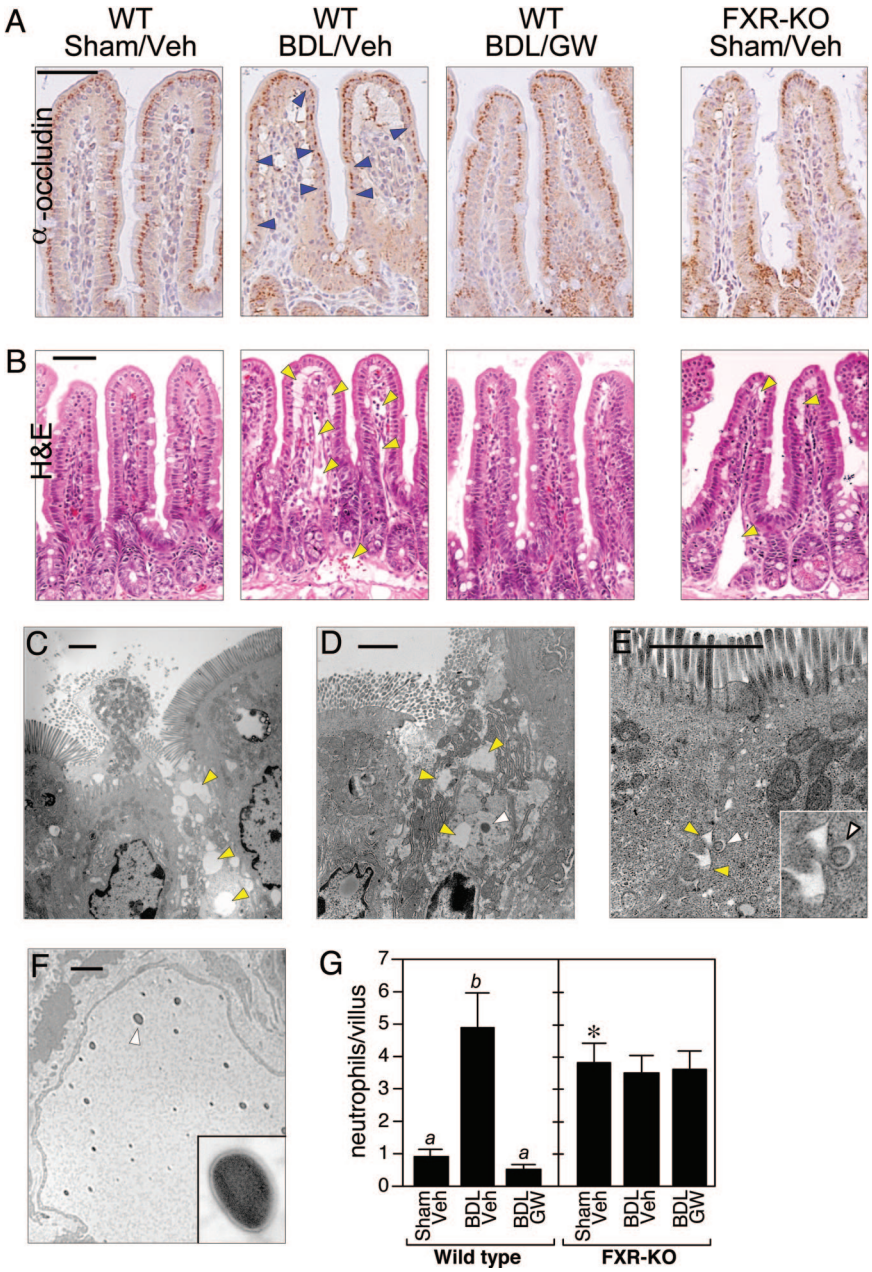

Fig. 4. FXR activation blocks mucosal injury. (*A* and *B*) Transverse sections of terminal ileum are shown for WT mice subjected to sham operation and vehicle treatment (WT/Sham/Veh), BDL and vehicle treatment (WT/BDL/Veh), or BDL and GW4064 treatment (WT/BDL/GW) and FXR-KO mice subject to sham operation and vehicle treatment (FXR-KO/Sham/Veh). The sections were immunostained with anti-occludin antisera (*A*) or stained with hematoxylin and eosin (H&E) (*B*). Occludin immunostaining (dark brown) is detected in the enterocytes of the villus epithelium. Notable examples of diminished occludin immunostaining are indicated by blue arrowheads in the WT/BDL/Veh section. Occludin immunostaining is drastically reduced in ileum from the FXR-KO/Sham/Veh mice. Edema and dilated lymphatic vessels are indicated by yellow arrowheads in hematoxylin and eosin (H&E)-stained sections. (Scale bars: 50 μm.) (*C–F*) Electron microscopy performed with sections of terminal ileum prepared from BDL WT mice (*C* and *D*) and sham-operated FXR-KO mice (*E* and *F*). *C–E* are oriented with the epithelial brush border at the top. Edema is indicated in *C–E* by yellow arrowheads. Bacteria in the mucosa are indicated in *D* and *E* by white arrowheads. (*E Inset*) A higher magnification of the bacterium and the surrounding edema. (*F*) Bacteria in the lymphatic vessels of a sham-operated FXR-KO mouse. (*Inset*) A higher magnification view of the bacterium indicated by the white arrowhead. (Scale bars: 2 μm.) (*G*) Neutrophils were quantified in transverse sections of terminal ileum prepared from WT and FXR-KO mice subjected to sham operation and vehicle treatment (Veh), BDL and vehicle treatment, or BDL and GW4064 (GW) treatment. Neutrophils were counted in 10 randomly chosen villi from four mice in each treatment group. The presence of different lowercase letters indicates statistical significance ($P < 0.05$) within each strain. The asterisk indicates statistical significance ($P < 0.01$) between sham-operated, vehicle-treated FXR-KO mice and sham-operated, vehicle-treated WT mice.

tion caused by biliary obstruction. No changes were seen in ileal rates of cell proliferation (assessed by immunostaining with Ki67 antibody) or apoptosis (assessed by TUNEL assays) in the different treatment groups (data not shown). Thus, FXR blocks the changes caused by BDL in WT mice without affecting cell proliferation or programmed cell death.

In marked contrast to the continuous occludin immunostaining seen in sham-operated WT mice, occludin staining was discontinuous and weak in FXR-KO mice, indicating a deterioration in the epithelial barrier even without BDL (Fig. 4*A*). Consistent with this result and the higher incidence of bacterial translocation in FXR-KO mice (Fig. 3*E*), bacteria and edema

were present in the junctions between epithelial cells in FXR-KO animals (Fig. 4*E*). Bacteria were also present in the dilated lymphatic vessels (Fig. 4*F*). These data demonstrate that the lack of FXR leads to mucosal injury and bacterial translocation even in the absence of additional insult. BDL did not exacerbate the edema (data not shown) or further increase the elevated neutrophil numbers (Fig. 4*G*) in the FXR-KO mice. Moreover, GW4064 administration had no effect on any of these parameters in FXR-KO mice (Fig. 4*G* and data not shown).

Summary and Perspectives

Biliary obstruction causes bacterial overgrowth and translocation in the small intestine that can be reversed by administration of bile acids (3, 4, 25–30). It has been proposed that the detergent properties of bile acids are responsible for their enteroprotective actions. Although bile acids were not assessed for direct antibacterial actions in this study, our data suggest a more sophisticated mechanism wherein activation of the bile acid receptor FXR protects against bacterial proliferation and its detrimental effects in the distal small intestine. The products of several genes regulated by FXR in ileum, including *Ang1*, *iNos*, and *Il18*, have established antimicrobial actions. It is not possible to tell from our data whether these genes are regulated by FXR in enterocytes or other cell types, including resident immune cells. The expression profile of *Ang1* as well as *Fgf15*, *Shp*, *Car12*, and *Ibabp* correlate well with FXR-mediated enteroprotection in the BDL model (Fig. 2), suggesting that the protective actions of FXR are likely to involve multiple downstream genes. Expression of *iNos* and *Il18* is more complex in that their expression is increased by BDL in both WT and FXR-KO mice (Fig. 2), which likely reflects their regulation by proinflammatory signaling cascades that are activated by BDL. Nevertheless, iNOS and IL18 may contribute to FXR-induced enteroprotection under physiologic or other pathophysiologic conditions. Notably, elevated concentrations of iNOS and IL18 are associated with mucosal damage and inflammatory bowel disease (21, 36). Regulation of these genes by bile acids, which are released from the gallbladder into the small intestine during feeding, may ensure an adequate level of enteroprotection during periods of increased microbial exposure while preventing the overproduction of proteins that can cause inflammation and intestinal disease.

In summary, our results demonstrate that FXR plays a crucial role in protecting the distal small intestine against bacterial overgrowth and the resulting disruption of the epithelial barrier. These findings raise the intriguing possibility that potent, synthetic FXR agonists may have therapeutic utility in patients with obstructed or reduced bile flow, including those on total parenteral nutrition, who are susceptible to bacterial overgrowth and translocation (37, 38).

Materials and Methods

Transcriptional Profiling Analysis. Total RNA was extracted from tissues by using RNA STAT-60 (Tel-Test, Friendswood, TX), and cDNA was prepared. Preparation of *in vitro* transcription products, oligonucleotide array hybridization, and scanning were performed by using Affymetrix high-density oligonucleotide array mouse genome 430A 2.0 chips according to Affymetrix protocols. To minimize discrepancies due to variables, the raw expression data were scaled by using Affymetrix MICROARRAY SUITE 5.0 software, and pairwise comparisons were performed. The trimmed mean signal of all probe sets was adjusted to a user-specified target signal value (200) for each array for global scaling. No specific exclusion criteria were applied. Additional analysis was performed by using the freeware program BULLFROG 7.

RTQ-PCR Analysis. Primers for each gene were designed by using PRIMER EXPRESS software (Applied Biosystems) based on GenBank sequence data. Primer sequences are available upon request. RTQ-PCRs (10 μl) contained 25 ng of cDNA, 150 nM of each primer, and 5 μl of SYBR Green PCR Master Mix (Applied Biosystems). All reactions were performed in triplicate on an Applied Biosystems Prism 7900HT Sequence Detection System, and relative mRNA levels were calculated by the comparative threshold cycle method by using cyclophilin as the internal control.

Animals and BDL. All experiments were performed on age-matched, male mice. WT mice, CYP27-KO mice (a gift from Eran Leitersdorf, Hadassah University Hospital, Jerusalem), and FXR-KO mice (a gift from Frank Gonzalez, National Institutes of Health, Bethesda) were maintained on a mixed-strain background (C57BL/6:129Sv). For transcriptional profiling studies, 3- to 4-month-old mice received a first dose of GW4064 (100 mg/kg in 1% Tween 80/1% methylcellulose) or vehicle by oral gavage followed by a second dose 12 h later. The mice were killed 14 h after the first dose, and the small intestine was removed, flushed with ice-cold saline, and cut into three segments of equal length representing the duodenum, jejunum, and ileum. The three segments were cut open longitudinally, and the mucosa were gently scraped and flash-frozen in liquid nitrogen. For BDL experiments, 8- to 10-month-old WT and FXR-KO mice were treated daily with GW4064 (100 mg/kg per day in 1% Tween 80/1% methylcellulose) or vehicle by gavage for 2 days before surgery and 5 days after. Animals treated with GW4064 or vehicle for 2 days were randomly assigned to BDL or sham-operated groups. Surgery was performed under general anesthesia through an upper midline abdominal incision. The common bile duct was mobilized and ligated by using 4/0 silk for the BDL group. Sham-operated mice had the same incision followed by mobilization of the common bile duct without ligation. All experiments were approved by the Institutional Animal Care and Research Advisory Committee at the University of Texas Southwestern Medical Center.

Serum Total Bilirubin Concentrations and Bacterial Counts. At the end of the BDL experiment, the mice were killed by halothane inhalation, blood was obtained from the inferior vena cava, and the ileum, cecum, and mesenteric lymph node complex were removed. The lumen of the ileum was washed with 1.5 ml of tryptic soy broth (Becton Dickinson), and the contents were collected. The cecum and mesenteric lymph node complex were weighed and homogenized in 1.5 ml of tryptic soy broth. Serial dilutions of ileal contents and cecal and mesenteric lymph node complex extracts were cultured on trypticase soy agar with 5% sheep blood plates (Becton Dickinson) under aerobic or anaerobic conditions. The numbers of colony-forming units were counted after incubation for 20 h at 37°C. Serum total bilirubin concentrations were measured by variation of the diazo method by using an Olympus Chemistry ImmunoAnalyzer in the Aston Pathology Laboratory at the University of Texas Southwestern Medical Center.

***In Situ* Hybridization.** *In situ* hybridization was performed on paraffin sections of ileum by using ^{35}S-labeled sense and antisense riboprobes against the FXR ligand binding domain (nucleotides 921-1380; GenBank accession no. U09416). Slides were exposed at 4°C for 14 days. In all cases, sections hybridized with the sense probe resulted in the absence of signal (data not shown).

Immunohistochemistry. Immunostaining was performed on deparaffinized transverse sections of ileum. Endogenous peroxidase activity was quenched with 0.3% H_2O_2. Nonspecific binding was blocked by incubating the sections for 30 min in 3% normal goat serum. The sections were incubated overnight with

rabbit anti-occludin antisera (Zymed) at a dilution of 1:800 at 4°C. The bound anti-occludin was detected by sequential incubation with a biotinylated goat anti-rabbit F(ab′)2 (Vector Laboratories) diluted at 1:200 followed by horseradish peroxidase-conjugated streptavidin (Vector Laboratories) at 1:500 dilution. Bound horseradish peroxidase–streptavidin was detected by addition of diaminobenzidine (DAKO).

Transmission Electron Microscopy. A 2- to 3-cm length of distal ileum was harvested, and the lumen was rinsed. The lumen was gently inflated with 2% glutaraldehyde in 0.1 M cacodylate buffer, and both ends were tied off with a suture. Further fixation was carried out at 4°C overnight. The tissues were postfixed in 1% osmium tetroxide in 0.1 M cacodylate buffer for 1 h, dehydrated in ethanol, and embedded in 812 resin. One-micrometer-thick survey sections were stained with 0.5% toluidine blue, and ultrathin sections were prepared from selected areas.

Statistical Analyses. All results are expressed as mean ± SEM. Statistical analyses were performed by using MINITAB RELEASE 13.3 software (Minitab, State College, PA). Multiple groups were tested by one-way ANOVA, followed by Fisher's least-significant-difference test for unpaired data, followed by the Mann–Whitney *U* test where appropriate. Comparisons of two groups were performed by using a Student *t* test. In cases where there was unequal variance (Bartlett's test) among groups, data were reevaluated after logarithmic transformation. A P value <0.05 was considered to be significant.

We thank Dr. Frank Gonzalez and Dr. Eran Leitersdorf for providing FXR-KO and CYP27-KO mice, respectively; Dr. Tim Willson and Patrick Maloney (both from GlaxoSmithKline, Research Triangle Park, NC) for GW4064; Dr. Ron Evans and Yuhua Zou for support and assistance in the microarray analysis; Dr. Christopher Gilpin, George Lawton, and the University of Texas Southwestern Molecular and Cellular Imaging Core Facility for assistance with electron microscopy and analysis; the University of Texas Southwestern Molecular Pathology Core Laboratory, Angie Bookout, and members of the S.A.K., D.J.M., and J.J.R. laboratories for technical assistance; Alisha Tizenor for assistance with graphics; and Drs. David Russell, Joe Goldstein, Ron Evans, and Lora Hooper for critically reading the manuscript. This work was funded by National Institutes of Health Grants DK067158 (to S.A.K.) and U19DK62434 (to S.A.K. and D.J.M.), the Robert A. Welch Foundation (S.A.K. and D.J.M.), and the Howard Hughes Medical Institute (A.M. and D.J.M.). D.J.M. is an Investigator of the Howard Hughes Medical Institute.

1. Russell, D. W. (2003) *Annu. Rev. Biochem.* **72,** 137–174.
2. Berg, R. D. (1995) *Trends Microbiol.* **3,** 149–154.
3. Ding, J. W., Andersson, R., Soltesz, V., Willen, R. & Bengmark, S. (1993) *Eur. Surg. Res.* **25,** 11–19.
4. Lorenzo-Zuniga, V., Bartoli, R., Planas, R., Hofmann, A. F., Vinado, B., Hagey, L. R., Hernandez, J. M., Mane, J., Alvarez, M. A., Ausina, V. & Gassull, M. A. (2003) *Hepatology* **37,** 551–557.
5. Cahill, C. J. (1983) *Br. J. Surg.* **70,** 590–595.
6. Cahill, C. J., Pain, J. A. & Bailey, M. E. (1987) *Surg. Gynecol. Obstet.* **165,** 519–522.
7. Evans, H. J., Torrealba, V., Hudd, C. & Knight, M. (1982) *Br. J. Surg.* **69,** 706–708.
8. Edwards, P. A., Kast, H. R. & Anisfeld, A. M. (2002) *J. Lipid Res.* **43,** 2–12.
9. Makishima, M., Okamoto, A. Y., Repa, J. J., Tu, H., Learned, R. M., Luk, A., Hull, M. V., Lustig, K. D., Mangelsdorf, D. J. & Shan, B. (1999) *Science* **284,** 1362–1365.
10. Grober, J., Zaghini, I., Fujii, H., Jones, S. A., Kliewer, S. A., Willson, T. M., Ono, T. & Besnard, P. (1999) *J. Biol. Chem.* **274,** 29749–29754.
11. Li, J., Pircher, P. C., Schulman, I. G. & Westin, S. K. (2005) *J. Biol. Chem.* **280,** 7427–7434.
12. Inagaki, T., Choi, M., Moschetta, A., Peng, L., Cummins, C. L., McDonald, J. G., Luo, G., Jones, S. A., Goodwin, B., Richardson, J. A., *et al*. (2005) *Cell Metab.* **2,** 217–225.
13. Forman, B. M., Goode, E., Chen, J., Oro, A. E., Bradley, D. J., Perlmann, T., Noonan, D. J., Burka, L. T., McMorris, T. & Lamph, W. W. (1995) *Cell* **81,** 687–693.
14. Rosen, H., Reshef, A., Maeda, N., Lippoldt, A., Shpizen, S., Triger, L., Eggertsen, G., Bjorkhem, I. & Leitersdorf, E. (1998) *J. Biol. Chem.* **273,** 14805–14812.
15. Maloney, P. R., Parks, D. J., Haffner, C. D., Fivush, A. M., Chandra, G., Plunket, K. D., Creech, K. L., Moore, L. B., Wilson, J. G., Lewis, M. C., *et al*. (2000) *J. Med. Chem.* **43,** 2971–2974.
16. Goodwin, B., Jones, S. A., Price, R. R., Watson, M. A., McKee, D. D., Moore, L. B., Galardi, C., Wilson, J. G., Lewis, M. C., Roth, M. E., *et al*. (2000) *Mol. Cell* **6,** 517–526.
17. Lu, T. T., Makishima, M., Repa, J. J., Schoonjans, K., Kerr, T. A., Auwerx, J. & Mangelsdorf, D. J. (2000) *Mol. Cell* **6,** 507–515.
18. Nathan, C. (1997) *J. Clin. Invest.* **100,** 2417–2423.
19. Wallace, J. L. & Miller, M. J. (2000) *Gastroenterology* **119,** 512–520.
20. Biet, F., Locht, C. & Kremer, L. (2002) *J. Mol. Med.* **80,** 147–162.
21. Reuter, B. K. & Pizarro, T. T. (2004) *Eur. J. Immunol.* **34,** 2347–2355.
22. Dyer, K. D. & Rosenberg, H. F. (2005) *Nucleic Acids Res.* **33,** 1077–1086.
23. Hooper, L. V., Stappenbeck, T. S., Hong, C. V. & Gordon, J. I. (2003) *Nat. Immunol.* **4,** 269–273.
24. Halmi, P., Lehtonen, J., Waheed, A., Sly, W. S. & Parkkila, S. (2004) *Anat. Rec. A Discov. Mol. Cell. Evol. Biol.* **277,** 171–177.
25. Deitch, E. A., Sittig, K., Li, M., Berg, R. & Specian, R. D. (1990) *Am. J. Surg.* **159,** 79–84.
26. Slocum, M. M., Sittig, K. M., Specian, R. D. & Deitch, E. A. (1992) *Am. Surg.* **58,** 305–310.
27. Ding, J. W., Andersson, R., Norgren, L., Stenram, U. & Bengmark, S. (1992) *Eur. J. Surg.* **158,** 157–164.
28. Ding, J. W., Andersson, R., Soltesz, V., Willen, R. & Bengmark, S. (1994) *J. Surg. Res.* **57,** 238–245.
29. Kalambaheti, T., Cooper, G. N. & Jackson, G. D. (1994) *Gut* **35,** 1047–1052.
30. Clements, W. D., Parks, R., Erwin, P., Halliday, M. I., Barr, J. & Rowlands, B. J. (1996) *Gut* **39,** 587–593.
31. Sinal, C. J., Tohkin, M., Miyata, M., Ward, J. M., Lambert, G. & Gonzalez, F. J. (2000) *Cell* **102,** 731–744.
32. Kleinert, H., Schwarz, P. M. & Forstermann, U. (2003) *Biol. Chem.* **384,** 1343–1364.
33. Manigold, T., Bocker, U., Traber, P., Dong-Si, T., Kurimoto, M., Hanck, C., Singer, M. V. & Rossol, S. (2000) *Cytokine* **12,** 1788–1792.
34. Parks, R. W., Stuart Cameron, C. H., Gannon, C. D., Pope, C., Diamond, T. & Rowlands, B. J. (2000) *J. Pathol.* **192,** 526–532.
35. Yu, Y., Sitaraman, S. & Gewirtz, A. T. (2004) *Immunol. Res.* **29,** 55–68.
36. Alican, I. & Kubes, P. (1996) *Am. J. Physiol.* **270,** G225–G237.
37. Holman, J. M., Jr., Rikkers, L. F. & Moody, F. G. (1979) *Am. J. Surg.* **138,** 809–813.
38. Garcia-Tsao, G. (2004) *Can. J. Gastroenterol.* **18,** 405–406.